Effect of surface curvature on magnetic moment and persistent currents in two-dimensional quantum rings and dots

D. V. Bulaev,* V. A. Geyler, and V. A. Margulis
Mordovian State University, Saransk 430000, Russia
(Received 25 August 2003; revised manuscript received 21 January 2004; published 25 May 2004)

The effect of the surface curvature on the magnetic moment and persistent currents in two-dimensional quantum rings and dots is investigated. It is shown that the surface curvature decreases the spacing between neighboring maxima of de Haas–van Alphen type oscillations of the magnetic moment of a ring and decreases the amplitude and period of Aharonov-Bohm type oscillations. In the case of a quantum dot, the surface curvature reduces the level degeneracy at zero magnetic fields. This leads to a suppression of the magnetic moment at low magnetic fields. The relation between the persistent current and the magnetic moment is studied. We show that the surface curvature decreases the amplitude and the period of persistent current oscillations.

DOI: 10.1103/PhysRevB.69.195313 PACS number(s): 73.20.At, 73.23.Ra, 75.75.+a

I. INTRODUCTION

A metallic ring of mesoscopic dimension in an external magnetic field is known to exhibit a wide variety of interesting physical phenomena: Aharonov-Bohm (AB) effects,[1,2] quantum Hall effects,[3] persistent currents,[4,5] the Berry phase,[6] and spin-orbit effects.[7]

One of the most important factors that cause complications in real experiments is the finite width of rings. Lorke and co-workers[8] showed that even in very small nanoscopic quantum rings, occupied with one or two electrons, there are some electron modes, corresponding to different radii of electron orbits in the ring. In a ring with finite width, not only are multiple channel effects important, but the penetration of the uniform magnetic field into the conducting region of the ring also plays a significant role.[4,5,9–11] For example, the penetration of a magnetic field into the conducting region can result in aperiodic oscillations of the persistent currents[2,4,9,10] and the breakdown of the simple linear relation between the persistent current and the magnetization.[4]

There are many theoretical models which take into account the finite width of rings,[4,5,9–11] such as the model of a two-dimensional (2D) ring with a hard-wall confinement potential,[5,12] a parabolic potential,[13,14] and a finite square-well potential.[15] Recently, the current-spin density-functional theory has been employed to study the combined effects of the confinement, Coulomb interactions, a spin polarization, and a magnetic field in a quantum dot and a quantum ring.[16,17] The above-mentioned models allow only numerical analysis. There are some exactly solvable models for 2D quantum rings.[4,9–11] Experiments on the spectroscopy of nanoscopic rings showed that a parabolic potential describes lowest electron states in a quantum ring very well.[8] Note that the confining potential proposed in Refs. 9 and 11 is in very good agreement with the experiment also.

Quantum interferences lead to a number of new phenomena in the transport properties of nanostructures. However, the phase coherence conservation of the electron wave functions in the whole sample can also affect the equilibrium properties of the system. Byers and Yang[18] were the first to show that an isolated normal-metal ring threaded by a magnetic flux carries an equilibrium current at finite temperature as long as the electron phase coherence is preserved. The work by Büttiker, Imry, and Landauer,[19] predicting persistent currents in 1D disordered loops, renewed the interest in the topic. This interest is heightened[4,20] by recent advances in submicrometer physics[21] that have brought the effect into reach of experimental investigation. It was shown that in very thin quantum rings the persistent current is a periodic function of the magnetic flux with a period $\Phi_0=hc/|e|$ (the AB effect). The persistent current I in this nanostructure is simply related to the magnetic moment M of the ring by $I=cM/S$, where S is the area of the ring. However, for a wide ring, in addition to orbital modes of electron motion in the ring there are also radial modes. Tan and Inkson[4] showed that the presence of the radial modes leads to aperiodicity and complication of oscillations of the persistent current in the ring. Moreover, in the wide quantum rings the effects of the penetration of magnetic field into the conducting region arise. These effects result in the breakdown of the linear relation between the persistent current and the magnetization[4] and the appearance of dHvA-type oscillations of the magnetization of the ring.[4,11,22]

In recent years, the effect of the surface curvature on the spectral, magnetic, and transport properties of nanostructures has attracted a substantial interest.[23–27] The recent progress in nanotechnology has made it possible to produce curved 2D layers[28] and nanometer-size objects of desired shapes.[29] In particular, an original technique developed in Refs. 28 and 29 enables fabricating nanotubes, quantum rolls, rings, and spiral-like strips of precisely controllable shapes and dimensions.

In this paper, we study the effect of surface curvature on the magnetic moment and persistent currents in a single isolated 2D quantum ring. Noninteracting spinless electrons in a 2D ring with a constant negative curvature are considered. The 2D ring is placed in an orthogonal magnetic field and an AB flux piercing through the center of the ring. The considered model of such a nanostructure is very flexible: both the radius and the width of the ring can be adjusted independently by suitably choosing the two parameters of the confining potential. Moreover, 1D rings and curved quantum dots can be described at peculiar values of the parameters. For the mathematical description of the considered system, we use a ring domain in a manifold of negative constant curvature (in mathematical literature also known as the Lobachevsky plane); for the geometric confinement of the ring, we choose a kind of the soft-wall potential (see the following section for details). It is significant that the problem of the physics on the surfaces of constant curvature has a deep relation with some interesting problems, like the quantum chaos,[30,31] influence of the negative curvature on the Berry phase,[32] and on the spectrum of the magneto-Bloch electron.[33] In recent years, the quantum Hall effect on the Lobachevsky plane is a subject of current interest.[24,34–36]

II. ELECTRON ENERGY SPECTRUM

Let us consider a two-dimensional electron gas on a surface L of constant negative curvature (the Lobachevsky plane) subjected to an orthogonal (to the surface) magnetic field that is the superposition of a uniform magnetic field $\mathbf{B}$ and the field of an Aharonov-Bohm solenoid with the flux Φ_{AB}. We employ the Poincaré realization for L identifying it with the complex disk $\{z\in\mathbb{C}:|z|<2a\}$ endowed with the metric

$$ds^2=\frac{dr^2+r^2d\varphi^2}{[1-(r/2a)^2]^2},$$

where a is the radius of curvature; (r,φ) are the polar coordinates in the plane $\mathbb{C}:z=r\exp(i\varphi)$ $(0<r<2a, 0\leqslant\varphi<2\pi)$.

The vector potential $\mathbf{A}$ may be represented as the sum of two terms: $\mathbf{A}=\mathbf{A}_1+\mathbf{A}_2$, where

$$\mathbf{A}_1=\left(0,\frac{Br}{2[1-(r/2a)^2]}\right)$$

is the vector potential of the uniform component and $\mathbf{A}_2=(0,\Phi_{AB}/2\pi r)$ is the vector potential of the AB flux.

The Hamiltonian of such a system is given by

$$H_0=\frac{\hbar^2}{2m^*a^2}\left\{-a^2\left[1-\left(\frac{r}{2a}\right)^2\right]^2\left[\frac{\partial^2}{\partial r^2}+\frac{1}{r}\frac{\partial}{\partial r}+\frac{1}{r^2}\left(\frac{\partial}{\partial\varphi}+i\frac{\Phi_{AB}}{\Phi_0}\right)^2\right]\right\}-i\frac{\hbar\omega_c}{2}\left[1-\left(\frac{r}{2a}\right)^2\right]\left(\frac{\partial}{\partial\varphi}+i\frac{\Phi_{AB}}{\Phi_0}\right)+\frac{m^*\omega_c^2a^2}{2}\left(\frac{r}{2a}\right)^2-\frac{\hbar^2}{8m^*a^2},\tag{1}$$

where m^* is the effective electron mass and ω_c is the cyclotron frequency. The last term in Eq. (1) is the surface potential[37] which arises from the surface curvature.[32]

We consider a 2D ring on L defined by a radial confining potential

$$V(r)=\lambda_1r^2+\frac{\lambda_2}{r^2}[1-(r/2a)^2]^2-V_0,\tag{2}$$

where λ_1,λ_2 are the parameters of the potential, $V_0=-\lambda_2/2a^2+2\sqrt{\lambda_2[\lambda_1+\lambda_2/(2a)^4]}$. The potential has the minimum $V(r_0)=0$ at

$$r_0=\left(\frac{\lambda_2}{\lambda_1+\lambda_2/(2a)^4}\right)^{1/4}.$$

Hence r_0 defines the average radius of the ring. It is easy to show, that for $r\simeq r_0$ the confining potential has the parabolic form

$$V(r)\simeq\frac{1}{2}m^*\omega_0^2(r-r_0)^2,$$

where the frequency $\omega_0=\sqrt{8[\lambda_1+\lambda_2/(2a)^4]/m^*}$ characterizes the strength of the transverse confinement.

The outer r_+ and inner r_- radii of the ring (and, therefore, its width $\Delta r=r_+-r_-$) can be expressed in terms of the Fermi energy E_F:

$$r_\pm=\left(\frac{V_0+E_F\pm\sqrt{2E_FV_0+E_F^2}}{2\lambda_1+\lambda_2/8a^4}\right)^{1/2}.$$

Note that in the limit of zero curvature. $(a\to\infty)$, the confinement potential (2) has the form

$$V(r)\underset{a\to\infty}{\longrightarrow}\lambda_1r^2+\frac{\lambda_2}{r^2}-2\sqrt{\lambda_1\lambda_2}.$$

As shown in Refs. 2, 4, 9, and 11, this potential provides a good description of the confinement for actual mesoscopic rings.

It is convenient to express the parameters of the confining potential in terms of r_0 and ω_0. Note that the model defined by Eq. (2) is very flexible. It can also be used to describe an 1D quantum ring $(r_0=\text{const},\omega_0\to\infty)$ and a 2D quantum dot $(r_0=0)$.

The Schrödinger equation for electrons on the surface of constant negative curvature with the confining potential defined by Eq. (2) reads

$$[H_0+V(r)]\psi(r,\varphi)=E\psi(r,\varphi).$$

By substituting the wave function $\psi(r,\varphi)=[\exp(im\varphi)/\sqrt{2\pi}]f_m(r)$ and by changing the variable $x=1/[1-(r/2a)^2]$, the Schrödinger equation is simplified to

$$(H_m-2m^*a^2E/\hbar^2)f_m(x)=0,$$

where

$$H_m=-\frac{d}{dx}x(x-1)\frac{d}{dx}+\frac{M^2}{4}\frac{1}{x-1}-\frac{m^{*2}\omega_m^2a^4}{\hbar^2}\frac{1}{x}+\frac{m^{*2}a^4}{\hbar^2}\left\{\omega_c^2+\omega_0^2\left[1-\left(\frac{r_0}{2a}\right)^2\right]^2\right\}-\frac{1}{4},\tag{3}$$

$$M=\sqrt{(m+\phi_{AB})^2+(m^*\omega_0 r_0^2/2\hbar)^2}, \tag{4}$$

$$\omega_m=\sqrt{[\omega_c-\hbar(m+\phi_{AB})/2m^*a^2]^2+\omega_0^2}, \tag{5}$$

$\phi_{AB}=\Phi_{AB}/\Phi_0$ is the number of Aharonov-Bohm flux quanta.

After some algebra we find that the spectrum of H_m consists of two parts: a discrete spectrum in the interval $(0,E_0)$ and a continuous one in the interval $[E_0,\infty]$, where $E_0=m^*\omega_c^2a^2/2+m^*\omega_0^2a^2[1-(r_0/2a)^2]^2/2$ is the lower bound of the continuous spectrum.

The discrete spectrum consists of finite numbers of eigenvalues

$$E_{nm}=\hbar\omega_m\left(n+\frac{1}{2}+\frac{M}{2}\right)+\frac{\hbar\omega_c}{2}(m+\phi_{AB})-\frac{m^*\omega_0^2r_0^2}{4}-\frac{\hbar^2}{2m^*a^2}\left[\frac{1}{2}(m+\phi_{AB})^2+\left(n+\frac{1}{2}\right)^2+\left(n+\frac{1}{2}\right)M\right], \tag{6}$$

where

$$n\in\mathbb{N}:0\leqslant n<m^*\omega_m a^2/\hbar-M/2-1/2. \tag{7}$$

The corresponding orthonormal eigenfunctions of H_m are given by

$$f_{nm}(x)=C_{nm}(x-1)^{\beta_m}x^{n-\alpha_m}F(-n,-n+2\alpha_m;2\alpha_m-2\beta_m-2n;1/x), \tag{8}$$

where $\alpha_m=\omega_m/\Omega, \beta_m=M/2$.

Using the properties of hypergeometric functions, one can find the normalization constants C_{nm}:

$$|C_{nm}|^2=2^{2\alpha_m-2\beta_m-2n-2}\frac{\Gamma(2\alpha_m-n)\Gamma(2\alpha_m-2\beta_m-n)}{a^2[\Gamma(2\alpha_m-2\beta_m-2n)]^2}\times\frac{(2\alpha_m-2\beta_m-2n-1)}{\Gamma(1+2\beta_m+n)n!},$$

where $\Gamma(x)$ is the Euler Γ-function.

The continuous spectrum of H_m is defined by

$$E_\nu=\frac{m^*\omega_c^2a^2}{2}+\frac{m^*\omega_0^2a^2}{2}[1-(r_0/2a)^2]^2+\frac{\hbar^2}{2m^*a^2}\nu^2,\quad \nu\in\mathbb{R}. \tag{9}$$

The corresponding orthonormal eigenfunctions are given by

$$f_{\nu m}(x)=C_{\nu m}x^{\alpha_m}(x-1)^{\beta_m}F(\alpha_m+\beta_m+i\nu+1/2,\alpha_m+\beta_m-i\nu+1/2;1+2\beta_m;1-x),$$

where

$$C_{\nu m}=\frac{(\sinh 2\pi\nu)^{1/2}}{2\pi a\Gamma(1+2\beta_m)}|\Gamma(-\alpha_m+\beta_m-i\nu+1/2)\times\Gamma(\alpha_m+\beta_m-i\nu+1/2)|.$$

As follows from Eq. (9), the lower bound of the continuous spectrum is a quadratic function of the uniform component of the magnetic field and independent of the AB flux. There is a finite number of discrete eigenvalues of H_m below this bound.

Note that the width of the quantum ring $\Delta r<r_0$ and for the quantum dot $\Delta r<2a$. Therefore, $E_F\ll m^*\omega_0^2a^2[1-(r_0/2a)^2]^2/2$ for these nanostructures. In this case, as can be seen from Eq. (9), the continuous spectrum is much higher than the Fermi energy for the quantum ring and dot. Hence, at low temperatures, there is no contribution of the continuous spectrum of electrons to magnetic and transport properties of these nanostructures.

As can be seen from Eq. (6), the effect of an AB flux on the energy spectrum and the wave function of electrons is to shift $m\rightarrow m+\phi_{AB}$. Note that, in contrast to the case of an 1D ring, an AB flux changes not only the phases of the wave functions but also the trajectory of electron states in a 2D quantum ring [see Eq. (8)], which results in a nonparabolic dependence of the energy spectrum on the AB flux.[9]

As can be seen from Eq. (6), the energy levels with the same quantum number n form a subband. The energy spectrum of the ring is a periodic function of Φ_{AB} with the period Φ_0. While the energy spectrum of the ring is an aperiodic function of B. Thus, the effect of the penetration of a magnetic field into the conducting region of the ring is to the appearance of the dependence of subband minima on a magnetic field and to the asymmetry of the subband dispersion about the subband minimum.[9] Note that the surface curvature leads to the additional subband asymmetry. In the following we consider the case of $\phi_{AB}=0$ only.

As can be seen from Eq. (6), at zero magnetic fields, the minima of all subbands are at $m=0$. At nonzero magnetic fields, all subband minima lie at $m=m_0$, where

$$m_0=\frac{m^*\omega_c r_0^2}{2\hbar[1-(r_0/2a)^2]}. \tag{10}$$

Note that, as for the case of the flat surface, m_0 is the number of quantum flux penetrated the ring with effective radius r_0.[9] The dependence of the subband minimum on the magnetic field is given by

$$E_{n,m_0}=\hbar\tilde{\omega}\left(n+\frac{1}{2}\right)-\frac{\hbar^2}{2m^*a^2}\left(n+\frac{1}{2}\right)^2, \tag{11}$$

where $\tilde{\omega}=\sqrt{\omega_c^2+\omega_0^2[1-(r_0/2a)^2]^2}$. Note that in the limit of zero curvature (the case of the flat surface) we get the following formula for the subband minimum:

$$E_{n,m_0}\underset{a\rightarrow\infty}{\longrightarrow}\hbar\omega\left(n+\frac{1}{2}\right), \tag{12}$$

where $\omega=\sqrt{\omega_c^2+\omega_0^2}$. Stress that in the case of a ring on the surface of constant negative curvature, $r_0<2a$; therefore the hybrid frequency $\tilde{\omega}$ is less than that corresponding to the case of the flat surface (ω). The surface curvature decreases the contribution of the term which is due to the ring width in $\tilde{\omega}$. Hence, the decrease of the transverse confinement of the ring is one of the manifestations of the surface curvature. As can be seen from Eq. (12), the spacing between the bottoms of neighboring subbands is $\hbar\omega$. From Eq. (11) it can be easily shown that for the case of the Lobachevsky plane this spacing is less than that for the flat surface and depends on the subband index. It can be seen from Eq. (11) that the bottoms of subbands are increasing with a magnetic-field. Moreover, the magnetic field dependence of the subband bottoms is stronger for the higher subbands. The decrease of the ring width shifts the subbands to higher energies, increases the subband spacings, and weakens the dependence of the subband bottom on a magnetic field. As can be seen from Eqs. (11) and (12), the surface curvature leads to the converse effects: the decrease of the curvature radius shifts the subbands to lower energies, decreases the subband spacings, and strengthens the dependence of the subband bottoms on a magnetic field.

Let us study the limiting cases. Firstly, we consider the case of an 1D ring $(r_0=\text{const},\omega_0\to\infty)$. The energy spectrum of the nanostructure at $\omega_0\to\infty$ can be found in the same way as in Ref. 9:

$$E_{n,m}=\hbar\tilde{\omega}\left(n+\frac{1}{2}\right)-\frac{\hbar^2}{2m^*a^2}\left(n+\frac{1}{2}\right)^2+\frac{\hbar^2}{2m^*r_0^2}\left[1-\left(\frac{r_0}{2a}\right)^2\right]^2(m-m_0)^2, \tag{13}$$

where m_0 is defined by Eq. (10). As can be seen from Eq. (13), electrons occupy the lowest subband only. The subband bottom is independent of a magnetic field and the subband energy spectrum is symmetric about m_0. Comparing Eq. (13) and that for the case of the flat surface, we find that the surface curvature shifts the subband minima to the lower magnetic field and weakens the magnetic field dependence of the electron energy.

Second, we consider the case of a quantum dot $(r_0=0)$. Assuming that $r_0=0$ in Eq. (6), we find the energy spectrum of electrons in a quantum dot on the surface of constant negative curvature,

$$E_{n,m}=\hbar\omega_m\left(n+\frac{1}{2}+\frac{|m|}{2}\right)+\frac{\hbar\omega_c m}{2}-\frac{\hbar^2}{2m^*a^2}\times\left[\frac{m^2}{2}+\left(n+\frac{1}{2}\right)^2+\left(n+\frac{1}{2}\right)|m|\right]. \tag{14}$$

It is well known[4] that the energy spectrum of an isotropic 2D quantum dot on the flat surface is degenerate at zero magnetic fields (the nth level is n-fold degenerate). The low magnetic field lifts the degeneracy of the levels, whereas, at high magnetic fields, the energy levels form the Landau subbands. As can be seen from Eq. (14), the surface curvature shifts the energy levels to the lower energy. Moreover, the shift is more essential for the levels with higher n or m. Furthermore, the surface curvature reduces the level degeneracy at zero magnetic fields. The level with $m=0$ is nondegenerate, whereas the levels with $m\neq 0$ are twofold degenerate. As can be seen from Eq. (14), the hybrid frequency ω_m depends on the quantum number m, therefore, for the levels with small $|m|$, the curvature has negligible effect on the behavior of the levels in magnetic fields. On the contrary, for the levels with large $|m|$, the curvature essentially changes the hybrid frequency and changes the behavior of the levels in a magnetic field.

III. MAGNETIC MOMENT

As is well known, the magnetic moment of any closed equilibrium thermodynamic system in an uniform magnetic field is defined by[38]

$$\mathcal{M}=-\left(\frac{\partial F}{\partial B}\right)_{T,N}=\sum_{n,m}\mathcal{M}_{n,m}f_0(E_{n,m}), \tag{15}$$

where F is the free energy, $f_0(E)$ is the Fermi distribution function, $N$is the number of electrons, and

$$\mathcal{M}_{n,m}=-\frac{\partial E_{n,m}}{\partial B} \tag{16}$$

is the magnetic moment of the (n,m)th state. The chemical potential of a system is determined completely by the normalization condition

$$N=\sum_{n,m}f_0(E_{n,m}).$$

Although we study the ring and the dot in a nonuniform magnetic field (orthogonal to the surface of constant negative curvature), the magnetic moment of the systems considered here is given by Eq. (15). In fact, an infinitesimal change δF in the free energy consequent on the infinitesimal change $\delta\mathbf{B}$ in a magnetic field is given by[39]

$$\delta F=-\int \mathbf{M}\delta\mathbf{B}dS,$$

where $\mathbf{M}$ is the magnetic moment of the unit area and dS is the surface element. In this work, the magnetic field is orthogonal to the surface: $\mathbf{B}=B\mathbf{n}$, where n is the normal to the surface. Therefore,

$$\delta F=-\delta\mathbf{B}\int \mathbf{M}dS=-\delta\mathbf{B}\mathcal{M},$$

where $\mathcal{M}$ is the magnetic moment of the system. Thus,

$$dF=-\mathcal{S}dT-\mathcal{M}d\mathbf{B}+\mu dN,$$

where $\mathcal{S}$ is the entropy of the system. It follows that the magnetic moment of the systems considered here is defined by Eq. (15). Note that the magnetic moment is given by this formula only for closed systems. In the case of open systems, as shown in Ref. 40, the magnetic moment is no longer de-

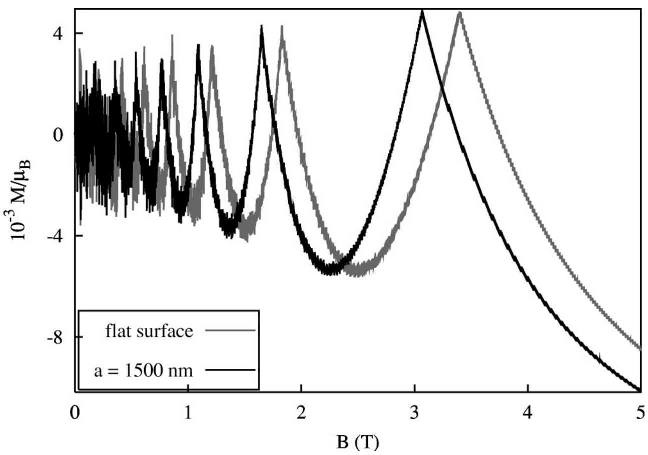

FIG. 1. The magnetic moment of a 2D quantum ring as a function of a magnetic field; $N=1000$, $r_0=800$ nm, $\omega_0=1.5\times10^{12}$ s^{-1}, $\phi_{AB}=0$, and $T=0$ K.

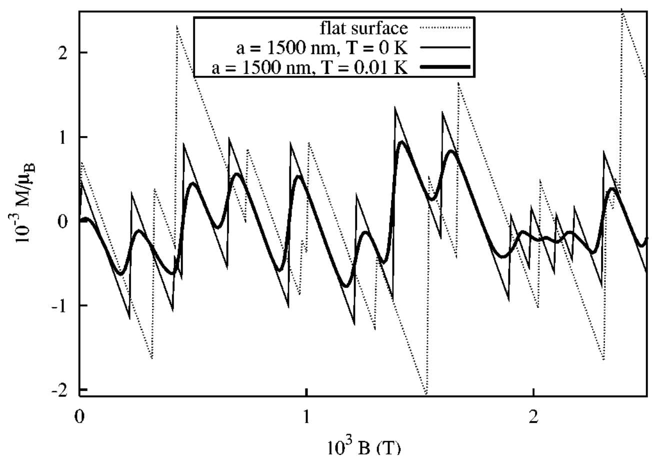

FIG. 2. The magnetic moment of a 2D quantum ring as a function of a magnetic field (the case of low magnetic fields); $N=1000$, $r_0=800$ nm, $\omega_0=1.5\times10^{12}$ s^{-1}, and $\phi_{AB}=0$.

fined by this formula. But in the case of the weak coupling between the system and reservoir, the magnetic moment can be calculated by Eq. (15).

For the case of a quantum ring on the Lobachevsky plane, substituting Eq. (6) into Eq. (16), we get

$$\frac{\mathcal{M}_{n,m}}{\mu_B}=-\frac{m_e}{m^*}\left[m+\phi_{AB}+\frac{\omega_c-\hbar(m+\phi_{AB})/2m^*a^2}{\omega_m}\times(2n+1+M)\right], \qquad (17)$$

where m_e is the free electron mass, and M and ω_m are defined by Eqs. (4) and (5) respectively.

As shown in Fig. 1, the magnetic moment of a 2D quantum ring on the Lobachevsky plane as well as on the flat surface[11,4] has a complex oscillation pattern: oscillations of the AB type are superimposed on oscillations of the de Haas–van Alphen (dHvA) type. The amplitude of AB-type oscillations is strongly suppressed by increasing magnetic-field strength, whereas the amplitude of dHvA-type oscillations is increased with the magnetic field. At low magnetic fields, the amplitudes of these oscillation types are of the same order of magnitude, and the superimposition of the oscillations leads to the appearance of a beating pattern in $\mathcal{M}(B)$ (Fig. 2). At high magnetic fields, the amplitude of AB-type oscillations is much smaller than that of dHvA-type oscillations (Fig. 1). Moreover, the AB-type oscillations are almost periodic in the strong-magnetic-field regime (Fig. 3).

Note that the AB-type oscillations of the magnetic moment arise from the electron-level crossings, whereas the dHvA-type oscillations arise from singularities in the electron density of states. It can be shown that the electron density of states is larger at the subband bottoms. Therefore, the maxima of dHvA-type oscillations arise when the chemical potential crosses the subband bottoms.

Let us consider the effect of the surface curvature on the magnetic moment of a ring. As mentioned above, the decrease of subband spacings is the one of manifestations of the surface curvature. This leads to the decrease of the spacing between neighboring maxima of dHvA-type oscillations (Fig. 1). Moreover, in the limit of low magnetic fields, the number of subbands below the Fermi energy is larger than that for the case of the flat surface. Therefore, the number of oscillations increases and the maximum of the amplitude of oscillations decreases with the increasing of surface curvature (Fig. 2).

The dependence of the hybrid frequency on the magnetic quantum number is the other manifestation of the surface curvature [Eq. (5)]. As follows from this equation that the surface curvature weakens the dependence of the energy levels on a magnetic field and decreases the level spacing. The former decreases the amplitude of AB-type oscillations, while the latter decreases the period of these oscillations (Fig. 3). As shown in Fig. 3, the monotonic part of the magnetic moment for a ring on the Lobachevsky plane is below that for the flat surface.

Note that temperature results in smearing of oscillation maxima and decreasing the oscillation amplitude (Fig. 2).

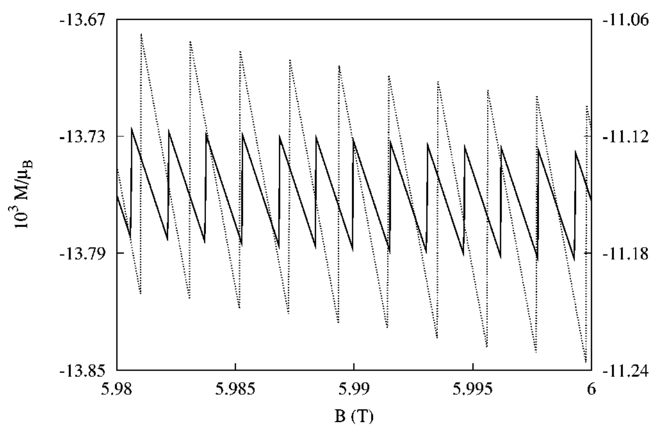

FIG. 3. The dependence of the magnetic moment of a 2D quantum ring on the magnetic field (the case of high magnetic fields). The magnetic moment of a 2D ring on the Lobachevsky plane with the radius of curvature $a=800$ nm is plotted with a solid line (left ordinate). The magnetic moment of a 2D ring on the flat surface is plotted with a dotted line (right ordinate); $N=1000$, $r_0=800$ nm, $\omega_0=1.5\times10^{12}$ s^{-1}, $\phi_{AB}=0$, and $T=0$ K.

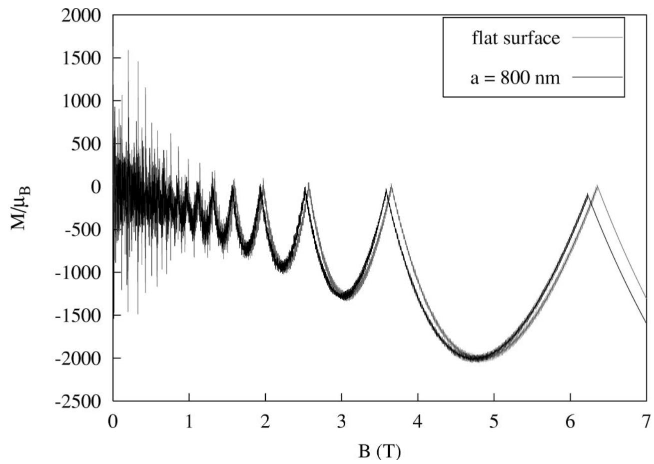

FIG. 4. The magnetic moment of a quantum dot as a function of a magnetic field; $N=500$, $\omega_0=1.5\times10^{12}$ s^{-1}, $\phi_{AB}=0$, and $T=0$ K.

Let us consider particular cases. In the limit of an 1D ring, substituting Eq. (13) into Eq. (16), we get for the magnetic moment

$$\frac{\mathcal{M}_{n,m}}{\mu_B}=\frac{m_e}{m^*}\left[1-\left(\frac{r_0}{2a}\right)^2\right]\left(m+\frac{\Phi_{AB}}{\Phi_0}-\frac{\Phi}{\Phi_0}\right), \quad (18)$$

where $\Phi=BS$ is the magnetic flux penetrating through a ring, and $S=\pi r_0^2/[1-(r_0/2a)^2]$ is the surface area circled by a ring with an effective radius r_0. As can be seen from this equation, the magnetic moment is a periodic function of the magnetic field with the period Φ_0. As follows from the analysis of the energy spectrum of electrons in an 1D ring, the surface curvature decreases the amplitude of the magnetic moment oscillations. Note that the dependence of the magnetic moment on the surface curvature is caused by the nonuniformity of a magnetic field. As mentioned above, we consider the case of an orthogonal (to the surface) magnetic field.

In the limit of a quantum dot, assuming that $r_0=0$ in Eq. (17), we obtain

$$\frac{\mathcal{M}_{n,m}}{\mu_B}=-\frac{m_e}{m^*}\left[m+\phi_{AB}+\frac{\omega_c-\hbar(m+\phi_{AB})/2m^*a^2}{\omega_m}\times(2n+1+|m+\phi_{AB}|)\right]. \quad (19)$$

As mentioned above, for the zero magnetic fields, the energy levels of an isotropic 2D quantum dot on the flat surface are highly degenerate. The low magnetic field lifts the degeneracy of the levels, and near the Fermi energy more electrons will occupy the states with $m<0$, which have a lower energy than the $m\geqslant0$ states. Therefore, the magnetic moment of the quantum dot on the flat surface has a large value at a weak magnetic field.[4] Further increase of the magnetic field leads to complex oscillations of $\mathcal{M}(B)$, which arise from the superimposition of the AB-type oscillations on the dHvA-type oscillations. In Fig. 4 we show the dependence

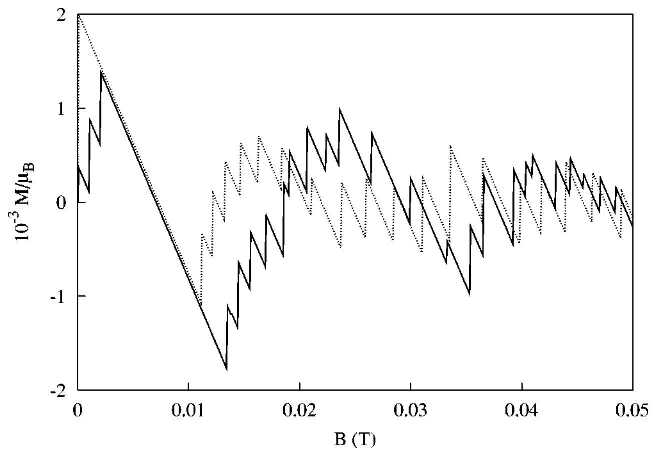

FIG. 5. The dependence of the magnetic moment of a quantum dot on a magnetic field (the case of low magnetic fields). The magnetic moment of a dot on the Lobachevsky plane with the radius of curvature $a=800$ nm is plotted with a solid line. The magnetic moment of a dot on the flat surface is plotted with a dotted line; $N=500$, $\omega_0=1.5\times10^{12}$ s^{-1}, $\phi_{AB}=0$, and $T=0$.

$\mathcal{M}(B)$ for the Lobachevsky plane as well as for the flat surface. As follows from the behavior of the electron levels in a magnetic field, the surface curvature decreases the period and the amplitude of the dHvA-type oscillations (Fig. 4). Since the surface curvature reduces the level degeneracy at zero magnetic fields, the magnetic moment of a quantum dot on the Lobachevsky plane is lower than that for the flat surface at weak magnetic fields. The new jumps in the field dependence of the magnetic moment arise with increasing the magnetic field, which are due to the crossings of degenerated levels at $B=0$ in the case of the flat surface (Fig. 5). At high magnetic fields, when the lowest subband is occupied only there is no level crossings, therefore the AB-type oscillations vanish (Fig. 6).

IV. PERSISTENT CURRENTS

Let us consider the persistent current of a 2D quantum ring on the Lobachevsky plane. We study the relation be-

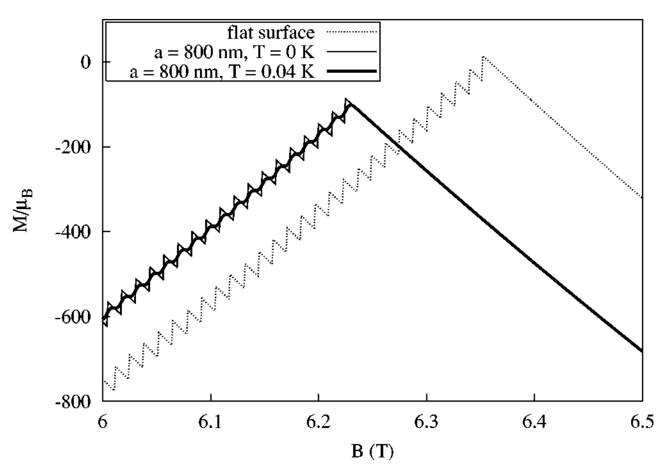

FIG. 6. The magnetic moment of a quantum dot as a function of a magnetic field (the case of a high magnetic fields); $N=500$, $\omega_0=1.5\times10^{12}$ s^{-1}, and $\phi_{AB}=0$.

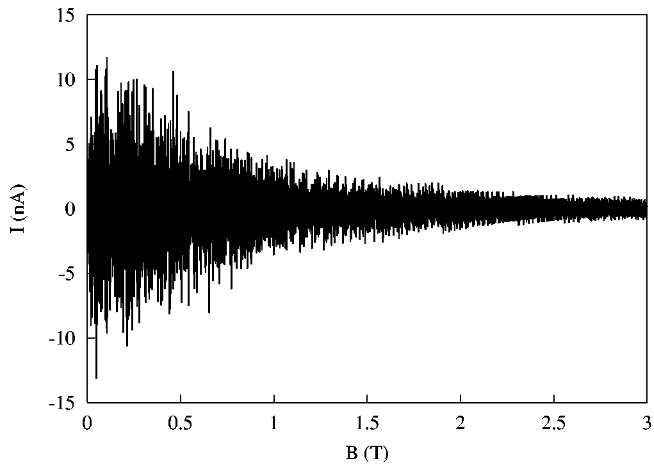

FIG. 7. The persistent currents of a 2D quantum ring on the Lobachevsky plane as a function of a magnetic field; $N=1000$, $a=1500$ nm, $r_0=800$ nm, $\omega_0=1.5\times 10^{12}\ \mathrm{s}^{-1}$, $\phi_{AB}=0$, and $T=0$ K.

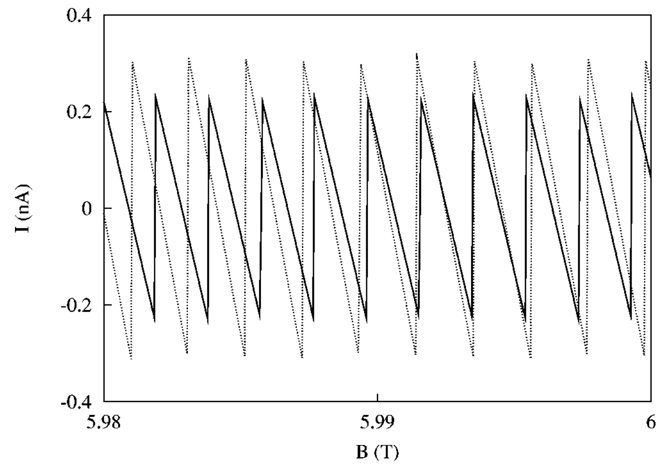

FIG. 8. The dependence of the persistent currents of a 2D ring on a magnetic field (the case of high magnetic fields). The persistent currents in a ring on the Lobachevsky plane with the radius of curvature $a=1500$ nm is plotted with a solid line. The persistent currents in a ring on the flat surface is plotted with a dotted line; $N=1000$, $r_0=800$ nm, $\omega_0=1.5\times 10^{12}\ \mathrm{s}^{-1}$, $\phi_{AB}=0$, and $T=0$ K.

tween the persistent current and the magnetic moment of the ring and we examine the effect of the surface curvature on the persistent current. Note that we take no account of the edge-state effects. In our model the Fermi energy is the same in the whole system, therefore, the inner and outer edge states contribute no current around the ring. When the wave functions of a system are zero at $r=0$, the persistent current can be calculated using the following equation:[18,41]

$$I=-c\left(\frac{\partial F}{\partial \Phi_{AB}}\right)_{T,N}=\sum_{n,m} I_{n,m} f_0(E_{n,m}), \qquad (20)$$

where

$$I_{n,m}=-c\frac{\partial E_{n,m}}{\partial \Phi_{AB}}. \qquad (21)$$

Taking into account Eq. (17), the persistent current of the (n,m)th state is given by

$$I_{n,m}=\frac{c}{\pi r_m^2}\left\{\mathcal{M}_{n,m}\left[1-\left(\frac{r_m}{2a}\right)^2\right]+\frac{m_e}{m^*}\mu_B\frac{\omega_c}{\omega_m}(2n+1)\right\}, \qquad (22)$$

where $r_m=\sqrt{2\hbar M/m^*\omega_m}$ is the effective radius of the state with quantum number m.[4,9] The first term in Eq. (22) is the classical current in a ring with a radius r_m in a magnetic field. The second term caused by the penetration of the magnetic field into the conducting region of the ring breaks the proportionality between the magnetic moment and the persistent current. It can be seen from Eq. (22) that only in the weak magnetic-field limit ($\omega_c \ll \omega_0$) the magnetic moment of an electron state is proportional to its current. In Fig. 7, we plot the persistent current as a function of a magnetic field. As can be seen from this figure, the persistent current shows rapid oscillations within the whole magnetic field range. The amplitudes of the persistent current are strongly suppressed by increasing magnetic-field strength. This is due to the fact that the oscillation amplitude $\sim\sqrt{P}$, where P is the number of the occupied subbands.[4] This number decreases with the magnetic field and this leads to the decrease of the oscillation amplitude. In the limit of low magnetic fields, there are some occupied subbands. The crossings of the highest occupied electron level with the levels of these subbands lead to the appearance of a beating pattern in $I(B)$. As mentioned above, in this magnetic-field regime, the persistent current is proportional to the magnetic moment. Therefore, the behavior of the persistent current is similar to the magnetic moment behavior (Fig. 2). In the strong magnetic-field regime, only the lowest subband is occupied and only the crossings of levels of this subband with the highest occupied level lead to oscillations of the persistent current. Since levels of the lowest occupied subband are nearly equidistant, the oscillations of the persistent current are nearly periodic in this magnetic-field regime (Fig. 8). The period of oscillations of the persistent current is the same as for the magnetic moment (Fig. 3). As mentioned above, the surface curvature decreases the period and the amplitude of oscillations of the magnetic moment. As can be seen from Eq. (22), the surface curvature leads to the additional decrease of the amplitude of oscillations of the persistent current with respect to the magnetic moment.

Note that Eq. (21) is also valid for electron states in a quantum dot, except for the states with $m+\phi_{AB}=0$. This is because, when $r_0=0$, the wave function of a state with $m+\phi_{AB}=0$ has a nonzero value at $r=0$, and Eq. (20) no longer applies. However, since Eq. (21) applies for all states if $r_0\neq 0$, the persistent current of the state with $m+\phi_{AB}=0$ can be obtained by taking the limit[4]

$$I_{n,-\phi_{AB}}=\lim_{r_0\to 0}\left[\lim_{m\to -\phi_{AB}} I_{n,m}\right]$$
$$=-\frac{|e|\omega_c}{4\pi}+\frac{|e|\hbar}{4\pi m^* a^2}\frac{\omega_c}{\omega}\left(n+\frac{1}{2}\right),$$

where $\omega=\sqrt{\omega_c^2+\omega_0^2}$.

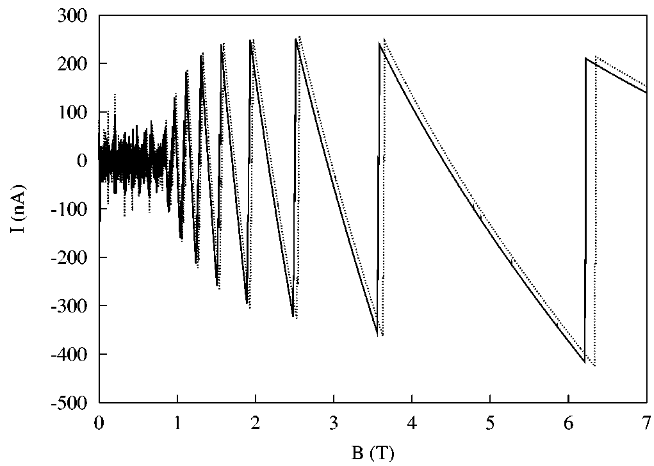

FIG. 9. The dependence of the persistent currents in a quantum dot on a magnetic field. The persistent currents of the dot on the Lobachevsky plane with the radius curvature $a=800$ nm is plotted with a solid line. The persistent currents of a dot on the flat surface is plotted with a dotted line; $N=500$, $\omega_0=1.5\times10^{12}$ s^{-1}, $\phi_{AB}=0$, and $T=0$ K.

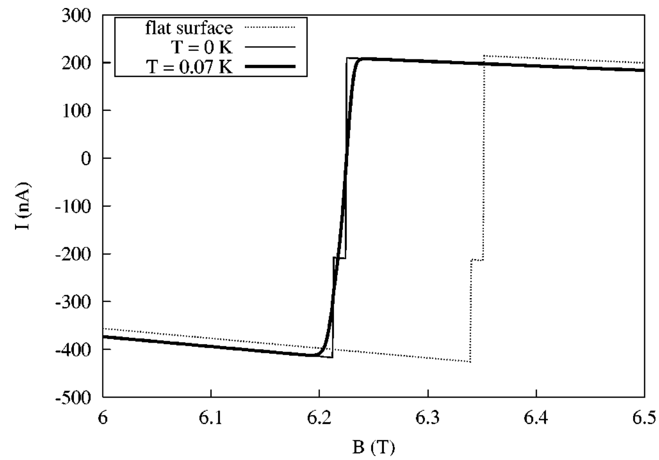

FIG. 10. The persistent currents of a quantum dot as a function of a magnetic field (the case of high magnetic fields); $N=500$, $a=800$ nm, $\omega_0=1.5\times10^{12}$ s^{-1}, and $\phi_{AB}=0$.

Note that the penetration of a magnetic field into the conducting region plays an essential role with increasing the magnetic field. This leads to the break of the proportionality between the magnetic moment and the persistent current of the quantum dot. The persistent current as a function of a magnetic field exhibits rapid jumps which appear when the Fermi energy crosses the subband bottoms (Fig. 9). The oscillations due to the level crossings with the highest occupied level are superimposed on these jumps. The amplitude of these oscillations decreases with a magnetic field. At high magnetic fields, this amplitude tends to zero (Fig. 10). As can be seen from Figs. 9 and 10, the surface curvature decreases the amplitude of the dHvA-type oscillations and shifts these oscillations in the low-field region.

V. CONCLUSIONS

The effect of the surface curvature on the magnetic moment and persistent currents of 2D quantum rings and dots is investigated. It is shown that the surface curvature decreases the subband spacings. This leads to decreasing of the spacing between neighboring maxima of de Haas–van Alphen type oscillations (Fig. 1). Moreover, the dependence of the hybrid frequency on the magnetic quantum number is the another manifestation of the surface curvature [Eq. (5)]. As follows from this equation, the surface curvature weakens the dependence of the energy levels on a magnetic field and decreases the level spacing. The former decreases the amplitude of Aharonov-Bohm-type oscillations, while the latter decreases the period of these oscillations (Fig. 3). Two limiting cases are considered: the case of an 1D quantum ring and the case of a quantum dot. It is shown that the surface curvature reduces the level degeneracy of a quantum dot at zero magnetic fields. Therefore, the magnetic moment of a quantum dot on the Lobachevsky plane is lower than that on the flat surface at weak fields. The persistent currents of a quantum ring and a quantum dot are studied. The relation between the persistent current and the magnetic moment of these nanostructures is investigated. It is shown that the surface curvature leads to the additional decrease of the amplitude of oscillations of the persistent current with respect to the magnetic moment.

ACKNOWLEDGMENTS

This work was supported by the INTAS Grant No. 00-257, the DFG-RAS Grant No. 436 RUS 113/572/0-2, the Russian Ministry of Education Grants Nos. E02-3.4-370 and E02-2.0-15, the RFBR Grants Nos. 02-01-00804 and 03-02-06006-mas.

*Electronic address: D.Bulaev@unibas.ch

[1] Y. Aharonov and D. Bohm, Phys. Rev. **115**, 485 (1959).
[2] U.F. Keyser, S. Borck, R.J. Haug, M. Bichler, G. Abstreiter, and W. Wegscheider, Semicond. Sci. Technol. **17**, L22 (2002).
[3] B.I. Halperin, Phys. Rev. B **25**, 2185 (1982).
[4] W.-C. Tan and J.C. Inkson, Phys. Rev. B **60**, 5626 (1999).
[5] Y. Avishai, Y. Hatsugai, and M. Kohmoto, Phys. Rev. B **47**, 9501 (1993).
[6] M.V. Berry and J.P. Keating, J. Phys. A **27**, 6167 (1994).
[7] Y. Meir, O. Entin-Wohlman, and Y. Gefen, Phys. Rev. B **42**, 8351 (1990).
[8] A. Lorke, R.J. Luyken, A.O. Govorov, J.P. Kotthaus, J.M. Garcia, and P.M. Petroff, Phys. Rev. Lett. **84**, 2223 (2000).
[9] W.-C. Tan and J.C. Inkson, Semicond. Sci. Technol. **11**, 1635 (1996).
[10] V.A. Margulis, A.V. Shorokhov, and M.P. Trushin, Physica E (Amsterdam) **10**, 518 (2001).
[11] E.N. Bogachek and U. Landman, Phys. Rev. B **52**, 14 067 (1995).
[12] S. Klama, J. Phys.: Condens. Matter **5**, 5609 (1993).
[13] T. Chakraborty and P. Pietiläinen, Phys. Rev. B **50**, 8460 (1994).
[14] J. Planelles, W. Jaskólski, and J.I. Aliaga, Phys. Rev. B **65**, 033306 (2002).
[15] I. Tomita and A. Suzuki, Phys. Rev. B **53**, 9536 (1996).
[16] A. Puente and L. Serra, Phys. Rev. B **63**, 125334 (2001).

[17] J.C. Lin and G.Y. Guo, Phys. Rev. B **65**, 035304 (2002).
[18] N. Byers and C.N. Yang, Phys. Rev. Lett. **7**, 46 (1961).
[19] M. Büttiker, Y. Imry, and R. Landauer, Phys. Lett. **96A**, 365 (1983).
[20] S. Viefers, P.S. Deo, S.M. Reimann, M. Manninen, and M. Koskinen, Phys. Rev. B **62**, 10 668 (2000).
[21] D. Mailly, C. Chapelier, and A. Benoit, Phys. Rev. Lett. **70**, 2020 (1993).
[22] V.A. Geyler, V.A. Margulis, and A.V. Shorokhov, Zh. Éksp. Teor. Fiz. **115**, 1450 (1999) [Sov. Phys. JETP **88**, 800 (1999)].
[23] C.L.S. Batista and D. Li, Phys. Rev. B **55**, 1582 (1997).
[24] A.L. Carey, K.C. Hannabuss, V. Mathai, and P. McCann, Commun. Math. Phys. **190**, 629 (1998).
[25] M.L. Leadbeater, C.L. Forden, T.M. Burke, J.H. Burroughes, M.P. Grimshaw, D.A. Ritchie, L.L. Wang, and M. Pepper, J. Phys.: Condens. Matter **7**, L307 (1995).
[26] M.V. Entin and L.I. Magarill, Phys. Rev. B **64**, 085330 (2001).
[27] D.V. Bulaev, V.A. Geyler, and V.A. Margulis, Phys. Rev. B **62**, 11 517 (2000).
[28] V.Y. Prinz, V.A. Seleznev, A.K. Gutakovsky, A.V. Chehovskiy, V.V. Preobrazhenskii, M.A. Putyato, and T.A. Gavrilova, Photonics Spectra **6**, 828 (2000).
[29] V. Y. Prinz, D. Grützmacher, A. Beyer, C. David, B. Ketterer, and E. Deccard, in *Proceedings of 9th International Symposium on Nanostructures: Physics and Technology*, edited by Zh. Alferov and L. Esaki (Ioffe Institute, St. Petersburg, Russia, 2001), p. 13.
[30] M.C. Gutzwiller, *Chaos in Classical and Quantum Mechanics* (Springer, New York, 1990).
[31] H.-J. Stöckmann, *Quantum Chaos: An Introduction* (Cambridge University Press, Cambridge, UK, 1999).
[32] S.A. Albeverio, P. Exner, and V.A. Geyler, Lett. Math. Phys. **55**, 9 (2001).
[33] J. Brüning and V.A. Geyler, Teor. Matem. Fiz. **115**, 368 (1999) [Theor. Math. Phys. **119**, 687 (1999)].
[34] R. Iengo and D. Li, Nucl. Phys. B **413**, 735 (1994).
[35] M. Alimohammadi and H.M. Sadjadi, J. Phys. A **29**, 5551 (1996).
[36] D.V. Bulaev, V.A. Geyler, and V.A. Margulis, Physica B **337**, 180 (2003).
[37] R.C.T. da Costa, Phys. Rev. A **23**, 1982 (1981).
[38] L.D. Landau and E.M. Lifshitz, *Statistical Physics* (Pergamon Press, Oxford, 1980), Part 1, p. 152.
[39] L.D. Landau and E.M. Lifshitz, *Electrodynamics of Continuous Media* (Butterworth-Heinemann, Oxford, 1998), p. 117.
[40] C. Benjamin and A.M. Jayannavar, cond-mat/0309133 (unpublished).
[41] F. Bloch, Phys. Rev. B **2**, 109 (1970).